

# Using excited states and degeneracies to enhance the electric polarizability and first hyperpolarizability

Ethan L. Crowell and Mark G. Kuzyk

*Department of Physics and Astronomy, Washington State University, Pullman, Washington 99164-2814*

We investigate the efficacy of boosting the nonlinear-optical response by using novel systems such as those in an excited state or with a degenerate ground state. By applying the Three Level Ansatz (TLA) and using the Thomas-Reiche-Kuhn (TRK) sum rules as constraints, we find the electric polarizability and first hyperpolarizability of excited state systems to be bounded, but *larger* than those derived for a system in the ground state. It is shown that a system with a degenerate ground state can have divergent intrinsic polarizabilities and that such divergences are real and not relics of a pathology in the perturbation theory. Furthermore, we demonstrate that these divergences only occur on time scales short compared to the relaxation time of the population difference to an equilibrium value. Such systems provide a way to get ultra-large nonlinear optical response. We discuss examples of huge enhancements in molecules and double quantum dots using a double quantum well as a model.

## I. INTRODUCTION

The interaction of a material with an electric field is often well described by the electric polarizability and hyperpolarizabilities. The polarizabilities derive from noting that the electric dipole moment  $\mathbf{p} = -e\mathbf{x}$  of a material will depend on the applied electric field  $\mathcal{E}$ . Doing a series expansion of the dipole moment in powers of the electric field leads to

$$p_i = \mu_i^{(0)} + \alpha_{ij}\mathcal{E}_j + \beta_{ijk}\mathcal{E}_j\mathcal{E}_k + \dots, \quad (1)$$

where  $\mu_i^{(0)}$  is the static dipole moment,  $\alpha$  is the polarizability tensor, and  $\beta$  is the first hyperpolarizability tensor [1, 2]. Equation 1 is in the frequency domain, but we will treat the static off-resonant limit. The polarizabilities are readily determined from

$$\alpha_{ij} = \left. \frac{\partial p_i}{\partial \mathcal{E}_j} \right|_{\mathcal{E}_j=0} \quad (2)$$

and

$$\beta_{ijk} = \frac{1}{1 + \delta_{j,k}} \cdot \left. \frac{\partial^2 p_i}{\partial \mathcal{E}_j \partial \mathcal{E}_k} \right|_{\mathcal{E}_j, \mathcal{E}_k=0}, \quad (3)$$

where  $\delta_{j,k}$  is the Kronecker delta.

Large (hyper)polarizabilities are important for a broad range of applications, including telecommunications [3], quantum computing [4, 5], three dimensional nanophotolithography [6, 7], and the development of materials for cancer therapies [8, 9]. As such, it is of interest to determine the fundamental characteristics that lead to large polarizabilities.

Such an investigation has been carried out [10, 11], beginning with the closed form expressions for the

off-resonant polarizability and first hyperpolarizability,

$$\alpha = 2e^2 \sum'_n \frac{x_{0n}x_{n0}}{E_{n0}} \quad (4)$$

and

$$\beta = 3e^3 \sum'_{n,m} \frac{x_{0n}\bar{x}_{nm}x_{m0}}{E_{n0}E_{m0}}, \quad (5)$$

where  $|0\rangle$  is the ground state vector,  $E_{nm} = E_n - E_m$ ,  $x_{nm} = \langle n|x|m\rangle$ ,  $\bar{x} = x - x_{00}$ , the prime on the sum indicates exclusion of the ground state from the sum, and the system's initial state is assumed to be  $|0\rangle$ . The above expressions are readily determined from time-dependent perturbation theory and apply for zero-frequency fields in the absence of damping, though they can be easily generalized to include oscillating fields and relaxation mechanisms [1, 2].

The upper bounds on the (hyper)polarizability is determined by applying the three-level ansatz (TLA) and using as constraints the Thomas-Reich-Kuhn (TRK) sum rules given by

$$\sum_n x_{pn}x_{nq} \left( E_n - \frac{1}{2}(E_p + E_q) \right) = \frac{N\hbar^2}{2m} \delta_{pq}, \quad (6)$$

where  $N$  is the number of electrons in the system. The limits obtained are [10, 11]

$$\alpha_{\max} = \frac{N_e e^2 \hbar^2}{m E_{10}^2} \quad (7)$$

and

$$\beta_{\max} = \sqrt[4]{3} \left( \frac{e\hbar}{\sqrt{m}} \right)^3 \left[ \frac{N^{3/2}}{E_{10}^{7/2}} \right]. \quad (8)$$

The energy difference between the ground and first excited state,  $E_{10}$ , sets a fundamental limit on

the electric polarizability and first hyperpolarizability. These limits have been corroborated by experiment [12], potential optimization [13–17], and calculations on quantum graphs [18–21] though a recent Monte Carlo study utilizing filtered sampling suggests that these limits may be an overestimate by approximately 30% [22].

It is important to reiterate that the above limits are for a system in its ground state. However, by optical pumping a system can be placed in an excited state. Indeed, it is known that the polarizability of a molecule can significantly increase with excitation [23–27]. Such a situation leads one to ask whether the polarizabilities of such systems—what we call the *excited state polarizabilities*—are bounded in the same sense as above, and whether the excited state polarizabilities can be larger than the aforementioned limits.

In this paper we seek to answer these questions. In section II, we apply the TRK sum rules to derive an upper bound on the excited state polarizabilities and we compare these limits to those of the ground state. This comparison will bring up the role of degenerate states on the polarizabilities, which will be discussed in section III. Finally, we treat an ensemble of degenerate systems and investigate the effects of relaxation processes.

## II. EXCITED STATE LIMITS

In this section we derive the limits on the polarizability and first hyperpolarizability for a system in the first excited state. We assume the absence of magnetic fields, which makes the hamiltonian invariant under time reversal and allows us to make the simplifying assumption that the dipole moment matrix is real valued.

### A. Linear response

The polarizability in the first excited state can be written as

$$\alpha = 2e^2 \sum_{n \neq 1} \frac{|x_{1n}|^2}{E_{n1}}. \quad (9)$$

This can be split into positive-definite and negative-definite terms

$$\alpha = 2e^2 \left( -\frac{|x_{01}|^2}{E_{10}} + \sum_{n>1} \frac{|x_{1n}|^2}{E_{n1}} \right). \quad (10)$$

To find a lower bound, we assume the transition moment in the negative-definite term,  $x_{10}$ , to be at

its maximum. This optimal value is defined via the  $p = q = 0$  sum rule:

$$\sum_n |x_{n0}|^2 E_{n0} = \frac{N\hbar^2}{2m} \quad (11)$$

$$\therefore |x_{10}|^2 \leq x_{\max}^2 = \frac{N\hbar^2}{2mE_{10}} \quad (12)$$

and requires  $x_{0n} = 0, \forall n > 1$ , which makes  $\alpha$  maximally negative. Note that the negative polarizability implies stimulated emission, as one finds for an inverted population as we have here.

Substituting these values of transition moments into Equation 9 gives the inequality

$$\alpha \geq -\frac{Ne^2\hbar^2}{mE_{10}^2}, \quad (13)$$

which according to Equation 7 is the negative of the limit for a ground state system.

We can likewise determine an upper bound on  $\alpha$  by placing all the oscillator strength in the positive terms. Exclusion of the negative terms from the SOS expression gives

$$\alpha \leq 2e^2 \sum_{n>1} \frac{|x_{1n}|^2}{E_{n1}}. \quad (14)$$

Recalling the  $p = q = 1$  sum rule

$$\sum_n |x_{1n}|^2 E_{n1} = \frac{N\hbar^2}{2m} \quad (15)$$

with  $x_{10} = 0$  gives

$$\sum_{n>1} |x_{1n}|^2 E_{n1} = \frac{N\hbar^2}{2m}. \quad (16)$$

Assuming that the transition between states 2 and 1 dominates – which gives the largest polarizability, Equation 14 can be rewritten using Equation 16 to yield

$$\alpha \leq \frac{Ne^2\hbar^2}{mE_{21}^2}. \quad (17)$$

Thus, the bounds of the polarizability for a system in its first excited state are given by

$$-\frac{Ne^2\hbar^2}{mE_{10}^2} \leq \alpha \leq \frac{Ne^2\hbar^2}{mE_{21}^2}. \quad (18)$$

Note that for a degenerate first excited state with  $E_2 = E_1$ , the limit diverges. This intriguing possibility for making arbitrarily-large polarizability is discussed later.

## B. Quadratic response

The limit of the first hyperpolarizability from an excited state parallels the original work [11, 28]. The first hyperpolarizability of the first excited state is given by

$$\beta = 3e^3 \sum'_{n,m} \frac{x_{1n}\bar{x}_{nm}x_{m1}}{E_{n1}E_{m1}}, \quad (19)$$

where we redefine the barring operator as  $\bar{x} = x - x_{11}$  and the prime now indicates exclusion of the first excited state from the sum. We can use the  $p = n, q = 1$  sum rule to get the excited state variant of the dipole-free SOS expression for  $\beta$  [29]:

$$\beta = -3e^3 \sum'_{n \neq m} x_{1n}x_{nm}x_{m1} \left( \frac{1}{E_{n1}E_{m1}} - \frac{2E_{n1} - E_{m1}}{E_{m1}^3} \right) \quad (20)$$

where, again, the prime on the sum indicates exclusion of the first excited state. Applying the TLA gives us

$$\beta = -3e^3 x_{10}x_{02}x_{21} \left( -\frac{2}{E_{21}E_{10}} + \frac{2E_{21} + E_{10}}{E_{10}^3} + \frac{2E_{10} + E_{21}}{E_{21}^3} \right) \quad (21)$$

Using the  $p = q = 0$  and the  $p = q = 1$  sum rules, the upper bound on the transition elements is [28]

$$\begin{aligned} |x_{01}x_{12}x_{20}| &\leq \frac{E}{\sqrt{1-E}} x_{10}^3 X \sqrt{1-X^4} \\ &\equiv \frac{E}{\sqrt{1-E}} x_{10}^3 \sqrt[4]{\frac{1}{3}} \sqrt{\frac{2}{3}} G(X), \end{aligned} \quad (22)$$

where the function

$$G(X) = \sqrt[4]{3} \sqrt{\frac{3}{2}} X \sqrt{1-X^4} \quad (23)$$

has as a maximum value  $G(\sqrt[4]{3}) = 1$ . Furthermore, from the  $p = q = 0$  sum rule we have

$$|x_{10}|^3 \leq \left( \frac{N\hbar^2}{2mE_{10}} \right)^{3/2}. \quad (24)$$

Putting this all together results in the inequality

$$\begin{aligned} |\beta| &\leq \frac{1}{2} \sqrt[4]{3} \left( \frac{e\hbar}{\sqrt{m}} \right)^3 N^{3/2} \\ &\quad \times \left( \frac{1}{E_{10}} + \frac{1}{E_{21}} \right)^{7/2} f(E), \end{aligned} \quad (25)$$

where we have defined  $E = \frac{E_{10}}{E_{20}} \leq 1$  and

$$\begin{aligned} f(E) &= -2E^2(1-E)^2 + 2E^4 + (1-E)E^3 \\ &\quad + 2(1-E)^4 + E(1-E)^3. \end{aligned} \quad (26)$$

Finally, it is easy to show that  $f(E)$  is bounded above by 2 and below by  $\frac{1}{4}$ , giving us a fundamental limit on the excited state polarizability:

$$\beta_{\max}^{\text{exc. st.}} = \sqrt[4]{3} \left( \frac{e\hbar}{\sqrt{m}} \right)^3 \frac{N^{3/2}}{E_{10}^{7/2}} \left( \frac{E_{20}}{E_{21}} \right)^{7/2}. \quad (27)$$

## C. Comparison to ground state limits

The excited state limits are compared with those derived for the ground state by normalizing them by the ground state limits to obtain the *intrinsic* excited state limits, yielding

$$-1 \leq \alpha_{\text{int}}^{\text{exc. st.}} \leq \left( \frac{E_{10}}{E_{21}} \right)^2 \quad (28)$$

$$-\left( \frac{E_{20}}{E_{21}} \right)^{7/2} \leq \beta_{\text{int}}^{\text{exc. st.}} \leq \left( \frac{E_{20}}{E_{21}} \right)^{7/2}. \quad (29)$$

Since  $E_{21} \leq E_{20}$ , the excited state hyperpolarizability limit is always at least as large as the ground state one, so the intrinsic excited state limit exceeds unity. The intrinsic excited state polarizability can also exceed unity, but not always. When the first and second excited states become degenerate, then both intrinsic values diverge. Thus, preparing a system in an excited state provides an opportunity for an intrinsic optical response much larger than what was previously thought possible based on the analysis of ground state systems.

## D. Monte carlo

Although the upper bound on the intrinsic values can be larger than unity, this does not imply that intrinsic values of actual systems will be. To determine the possibility of intrinsic values greater than one, we implement a statistical approach in which we randomly generate sets of eigenenergies and transition moments. The moments and energies are chosen such that the diagonal sum rules are obeyed exactly, while the off-diagonal sum rules are obeyed to within a standard error  $\epsilon$ . The technique for choosing such sets has been described elsewhere [22].

Fig 1 plots the intrinsic excited state limits for Monte-Carlo-generated "molecules" (points) and the intrinsic limits given by Equations 28 and 29 (line) as a function of the energy ratios. The excited state

intrinsic polarizabilities and hyperpolarizabilities are much larger than unity, and larger values of  $E_{10}/E_{21}$  tend to give larger intrinsic values, in agreement with Equations 28 and 29. Also, all points are seen to fall below the limit line, so the calculated limits are obeyed.

As the energy ratio  $E_{20}/E_{21}$  becomes large, the points fall lower below the calculated limits, implying that they overestimate the response when the excited states become degenerate. Such behavior is familiar when the the sum rules are truncated, as is done in applying the TLA. This can lead to unphysical behavior[30] and give rise to a gap between the limit and physical systems [22]. Whether this is the case here, or if this apparent gap is just the result of under-sampling due to limited computation time is currently unknown and will be the subject of future studies.

We stress that intrinsic quantities are not the sole focus for optimization, but rather are an intermediate step in finding materials that scale in a way that optimizes the raw values. A pitfall to the approach of optimizing the intrinsic polarizabilities is that, although large intrinsic values can result from large excited state polarizabilities, they can also result from small polarizabilities provided sufficiently small ground state limits. However, this appears not to be the case with the excited state polarizabilities as illustrated in Fig 2; large intrinsic values can also correspond to large unscaled values that are enhanced many orders of magnitude over what is possible in the ground state.

An interesting example of large polarizability of an excited-state system is the Rydberg atom, where one of the valence electrons is excited to a large principle quantum number. The atoms are surprisingly stable due to the negligible overlap of the excited states with the lower lying states [31]. It is known that Rydberg atoms tend to have very large polarizabilities, varying as  $n^7$ , where  $n$  is the principle quantum number [32]. Because  $n$  is quite large for Rydberg atoms (upwards of 30), the polarizabilities can reach values on the order of  $10^{12} a_0^3$  [33–35].

To illustrate the enhancement experienced by Rydberg atoms, we consider Rubidium. In the ground and first excited states, the valence electron occupies the  $^2S_{1/2}$  and  $^2P_{1/2}$  orbitals, respectively, with energies given in Table I. Hence, the ground state limit for Rubidium is

$$\begin{aligned} \alpha_{max} &= \frac{e^2 \hbar^2}{m E_{10}^2} \\ &= 2.25688 \times 10^8 a_0^3, \end{aligned} \quad (30)$$

where we have assumed, for simplicity, that only the excited valence electron interacts with the field. The polarizability for Rubidium has been measured

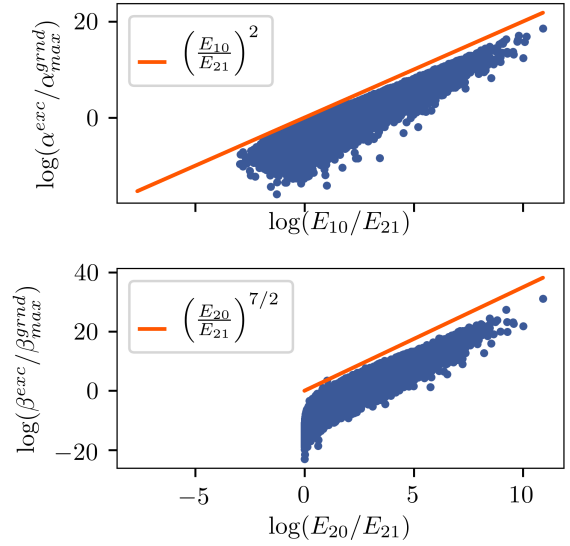


FIG. 1. Intrinsic excited state polarizabilities as function of energy parameter. The orange line indicates the limits derived in the previous section and the blue points are the values obtained from randomly generating energies and transition moments. One can see that the limits are well obeyed.

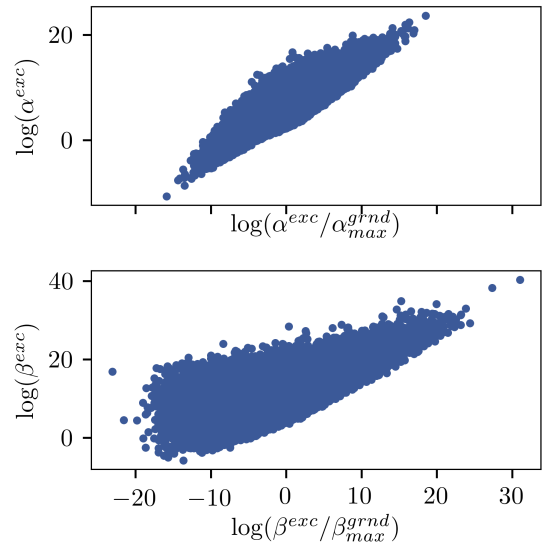


FIG. 2. Unscaled vs intrinsic polarizabilities. The fact that the polarizabilities can have large scaled and unscaled values assures that we are not simply minimizing the maximum ground state response when seeing large intrinsic values.

Level	Energy ( $E_h$ )	Polarizability ( $a_0^3$ )	Ref.
$^2S_{1/2}$	0.000	$3.20 \times 10^2$	[36, 37]
$^2P_{1/2}$	0.0000665649		[36]
$50^2S_{1/2}$	0.000178040	$2.03 \times 10^{11}$	[33, 36]
$48^2S_{1/2}$	0.000178019		[36]
$50^2P_{1/2}$	0.000178026	$1.19 \times 10^{12}$	[33, 36]
$49^2S_{1/2}$	0.000178028		[36]

TABLE I. Energy levels and static polarizabilities for Rubidium.

and calculated for excited states up to  $n = 50$ , with some characteristic values shown in Table I. Thus, the intrinsic polarizability for Rubidium  $50^2P_{1/2}$  is  $5.27 \times 10^3 a_0^3$ , much larger than the limit of unity for ground state systems. Although the states pertinent to the dynamics of a Rydberg atom's optical response are not the ground, first, and second excited states treated above, we still see the same trend: by exciting to a higher energy state where the energy levels are more dense, one can exceed the fundamental limits placed on the ground state polarizabilities.

We can compute the excited state limit if we make the associations  $E_1 \rightarrow E_n = 50^2P_{3/2}$ ,  $E_2 \rightarrow E_{n-1} = 49^2S_{1/2}$ , and  $E_0 \rightarrow E_{n+1} = 48^2S_{1/2}$ . Note that  $48^2S_{1/2}$  and  $49^2S_{1/2}$  are associated with  $E_0$  and  $E_2$  because they are the closest adjacent energy levels to  $50^2P_{3/2}$  with a nonzero electric dipole transition moment with it. The excited state limit for  $50^2P_{3/2}$  is then seen to be  $1.89 \times 10^{18} a_0^3$ , which is still well above the reported value.

Based on the analysis presented in this section, it is highly likely that molecules exist with an unremarkable hyperpolarizability, but when excited may have an ultra-large hyperpolarizability if that excited state is nearly degenerate.

### III. ROLE OF DEGENERATE STATES

In the previous section we saw that a near degeneracy can enhance the polarizabilities. To investigate this enhancement, we compute the polarizability using finite fields and compare to the perturbative treatment for a double-well potential. That analysis provides insights into the physics of the divergence. Finally, we will investigate the effects of interactions and the relaxation mechanisms. For simplicity we will focus our discussion entirely on the role of degenerate states and thus assume the system to be in a ground state that's quasi-degenerate with the first excited state.

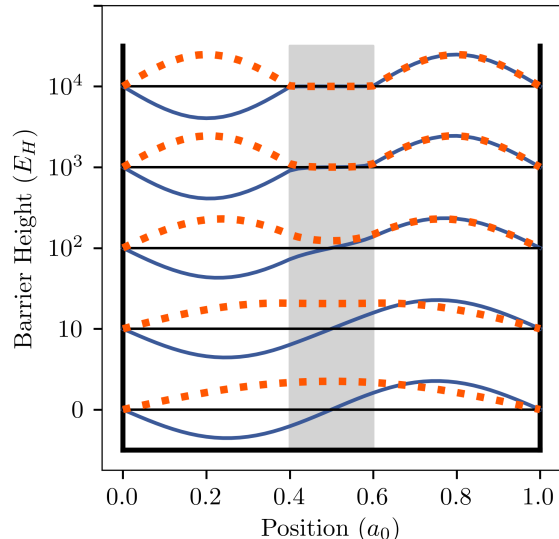


FIG. 3. Two lowest energy eigenfunctions as a function of barrier height. As the barrier height increases, the eigenfunctions inside the barrier become suppressed and the states approach degeneracy.

#### A. Finite fields

We numerically simulate the optical response of an electron in an infinite well of width  $L$  with a rectangular barrier in the middle of variable height but with fixed width  $d$ . The time independent Schrödinger equation for the system is, in atomic units,

$$-\frac{1}{2}\nabla^2\psi(x) + V(x)\psi(x) = E\psi(x), \quad (31)$$

where the potential is

$$V(x) = \begin{cases} 0, & 0 < x < \frac{L-d}{2} \\ V_0, & \frac{L-d}{2} < x < \frac{L+d}{2} \\ 0, & \frac{L+d}{2} < x < L \\ \infty, & \text{otherwise.} \end{cases} \quad (32)$$

The eigenenergies and eigenfunctions are determined by applying the finite difference technique to the spatial domain and diagonalizing the resulting matrix expression for the Hamiltonian. Fig 3 shows the eigenfunctions for various barrier heights. As the barrier height increases, the wavefunction inside the barrier becomes suppressed, resulting in the ground and first excited state curvatures on both sides to become identical. Hence, the two states become degenerate as the barrier height approaches infinity.

The first step in the finite fields method is to compute the induced dipole moment  $p$  for a large number

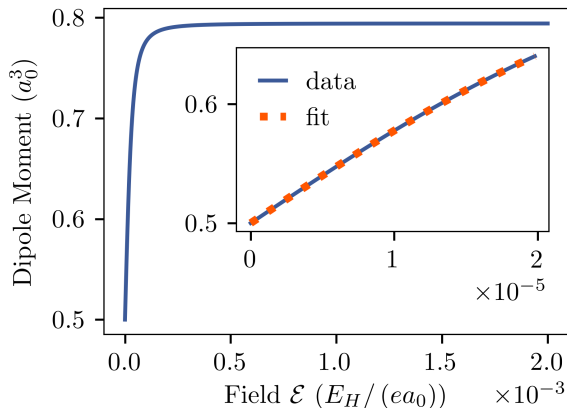


FIG. 4. Induced electric dipole moment as a function of electric field strength. In the inset, the orange dotted line shows the polynomial fit.

of electric field strengths  $\mathcal{E}$ , resulting in a numerical representation of the function  $p(\mathcal{E})$ . An example of this function for a barrier height of  $2000 E_H$  can be seen in Fig 4. Note that as the field strength increases, the induced dipole moment appears to saturate at  $0.8 a_0^3$ , which corresponds to the particle being localized in the right well. At infinite field strength the dipole moment saturates at  $1 a_0^3$  due to the particle's inability to penetrate the infinite walls on either side of the box.

With the function  $p(\mathcal{E})$  in hand, one can fit it with a polynomial (orange dotted line in the figure) and determine the polarizabilities by comparison with Equation 1. This procedure is repeated for several barrier heights. For comparison, we use the states for zero field to compute the SOS expression for  $\alpha$ , Eq 4. The results are shown in Fig 5.

There is excellent agreement between the finite fields method and the perturbation method, and both methods diverge as the system approaches degeneracy. This suggests that these large polarizabilities are real and not just the result of perturbation theory breaking down. Indeed, the physical origin of the divergence can be readily elucidated. Fig 6 shows the ground state wavefunction for zero field – where we have assumed the electron to be delocalized – and for an infinitesimal field, where the ground state is unique. It is seen that the electron immediately localizes upon application of the field. This corresponds to a nearly discontinuous change in the mean position of the electron which, in light of Eq 2, implies a truly divergent polarizability.

It is important to note that the divergence is not present at degeneracy. For infinite barrier height, the delocalized state cannot tunnel through the barrier, preventing the electron from occupying the

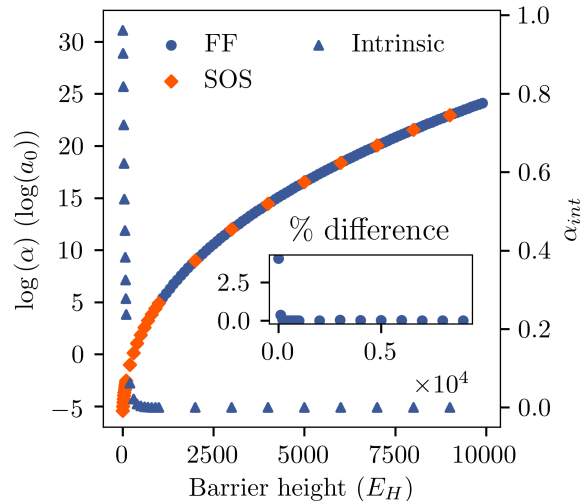


FIG. 5. Polarizability as a function of barrier height. The polarizability is seen to diverge as the barrier height increases and the system approaches degeneracy, while the intrinsic polarizability approaches zero. The divergence is present in both the perturbative and finite fields calculations, suggesting that it is a real effect. The inset shows the percent difference between the finite fields and perturbative treatments.

ground state of the perturbed system. Indeed, the time it takes the electron to tunnel through the barrier is inversely proportional to the energy difference between the two states. The energy difference between the states is unchanged to first order in perturbation theory, whence we find the time to tunnel  $\tau$  is

$$\tau = \frac{1}{E_{10}}. \quad (33)$$

Thus, the response time also diverges. Indeed, the intrinsic polarizability  $\alpha/\alpha_{\max}$  goes to zero as the barrier height becomes infinite, and thus we can conclude that the response time diverges more quickly than the polarizability. If we recall that the figure of merit (FOM) for the electric polarizability can be defined as the polarizability divided by the response time, we see that although the polarizability diverges, the FOM remains finite.

## B. Effects of damping

The above calculations only treat a single electron, isolated from any outside interactions. We would like to include relaxation mechanisms into the dynamics to determine whether the aforementioned divergences are physically feasible. As such, it is

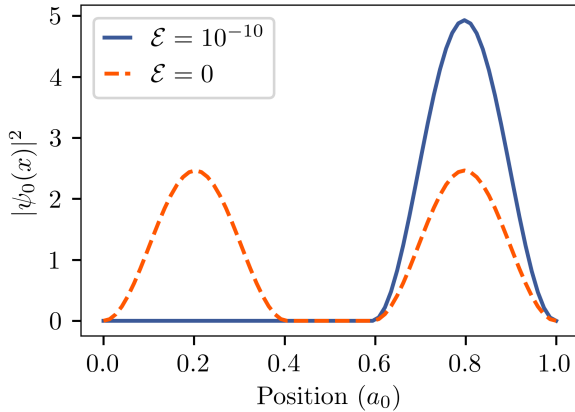


FIG. 6. Ground state wavefunction before and after application of an infinitesimal field. Note the discontinuous jump of the mean position of the electron from  $0.5 a_0$  to  $0.8 a_0$ , which corresponds to a divergent polarizability. The data was taken for a field strength of  $\mathcal{E} = 1 \times 10^{-10} E_H/(ea_0)$ .

pertinent to investigate the behavior of an *ensemble* of such near degenerate systems. Before doing so, however, we will first treat a single electron in the presence of damping.

### 1. Single electron with damping

To include damping into the single electron scheme, one effectively lets  $E_{n0} \rightarrow E_{n0} - i\gamma_{n0}$  in Eq 4, where  $\gamma_{n0}$  describes the relaxation mechanisms. The most natural choice of damping parameter is that deriving from Fermi's Golden Rule. That is, the natural linewidth

$$\begin{aligned} \gamma_{nm} &= \frac{1}{\hbar} \Gamma_{nm} \\ &= \frac{2}{3\hbar} \left( \frac{\Omega_{nm}}{c} \right)^3 e^2 |x_{nm}|^2. \end{aligned} \quad (34)$$

This term typically prevents the denominator from vanishing and results in a complex but finite polarizability. Inclusion of damping, however, has a minimal effect on the divergence seen above because of the form of Eq 34. As the system approaches degeneracy, the damping term approaches zero faster than the energy difference, as illustrated in Fig 7.

### 2. Dynamics of an Ensemble

The dynamics of an ensemble have been treated before [1] and are well known. Assuming we are suffi-

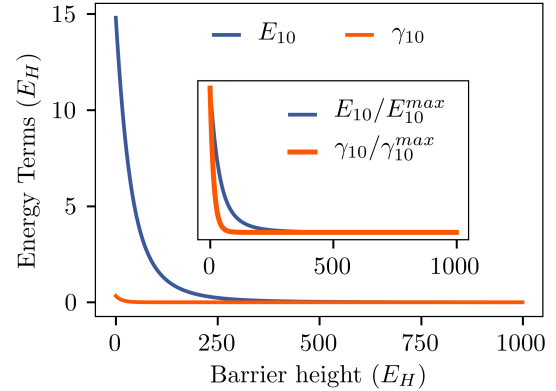


FIG. 7. The pertinent energy difference  $E_{10}$  along with the corresponding damping term  $\gamma_{10}$ . The damping term approaches zero in the degenerate limit more quickly than does the energy difference, thereby not suppressing the divergence of the polarizabilities.

ciently close to degeneracy that only the ground and first excited state matter, we can treat the system as consisting of only two levels. The steady-state result for the zero-frequency susceptibility—to all orders—is [1]

$$\chi = -\frac{N(\rho_{11} - \rho_{00})^{(eq)} |\mu_{10}|^2 (\Omega_{10} + i/T_2) T_2^2 / \hbar}{1 + (\omega_{10})^2 T_2^2 + (4/\hbar^2) |\mu_{10}|^2 |\mathcal{E}|^2 T_1 T_2} \quad (35)$$

where  $\Omega_{10} = E_{10}/\hbar$  is the resonant frequency between the two states and the relaxation processes are described by time constant  $T_1$ , the characteristic time at which the population difference  $(\rho_{11} - \rho_{00})$  decays to its equilibrium value, and  $T_2$ , the dipole dephasing time between the two states. If we treat the optical field as a reservoir with which the ensemble can exchange energy we can apply the canonical ensemble to compute the probability of being in a given state. The probability  $P_i$  of occupying a state with energy  $E_i$  is given by the well known expression [38]

$$P_i = \frac{e^{-\beta E_i}}{\sum_j e^{-\beta E_j}}, \quad (36)$$

where  $\beta = 1/kT$ . For a degenerate two-level system, this reduces to

$$P_{1,2} = \frac{1}{2}. \quad (37)$$

which leads to the result

$$(\rho_{11} - \rho_{00})^{(eq)} = 0. \quad (38)$$

We see that the steady state response is zero. Thus, the system will only have a large optical response when there is nonzero population difference between the degenerate states; that is, as long as the relaxation processes are very slow compared to the time of the experiment.

#### IV. CONCLUSION

In summary, a divergent upper limit of the excited state polarizabilities that exceeds the well-known ground state limits has motivated the above studies to determine whether this enhancement effect can be applied to real systems. A filtered monte carlo algorithm shows that it is physically feasible for an excited state system to have an intrinsic polarizability greater than unity, thus beating the ground state limit. The finite field method demonstrates that the divergent polarizabilities are not simply the result of a misapplication of perturbation theory but are physical in nature on short time scales. Finally, we

have shown that the polarizability can be enhanced by exciting a molecule and these enhancements originate in the near degeneracy of highly-excited states that near the continuum band. Similarly, a system with a degenerate ground state also shows a divergent response; a double quantum well is shown to behave in this way. These results suggest several avenues for enhancing the nonlinear-optical response in common systems.

In particular, this work suggests the design of new molecules made of two sub-units that are weakly interacting to mimic the particle in a box with a large central barrier. The difficulty of this approach may be in forcing the system into a ground state where one electron is delocalized over the two sub units. Alternatively, artificial structures such as nanowires with defects or double quantum dots [39, 40] may be simpler to fabricate as long as their response is quantum in nature, requiring either low temperature or small structures. While challenges may persist, these observations demonstrate that there are ways to trick nature into getting ultra large nonlinear response, which can be put to use in new devices.

- 
- [1] R. W. Boyd, *Nonlinear Optics*, 3rd ed. (Academic Press, 2009).
  - [2] M. G. Kuzyk, *Nonlinear Optics: A Student's Perspective* (2017).
  - [3] Q. Y. Chen, L. Kuang, Z. Y. Wang, and E. H. Sargent, *Nano. Lett.* **4**, 1673 (2004).
  - [4] I. Chuan and Y. Yamamoto, *Phys. Rev. A* **52**, 3489 (1995).
  - [5] G. D. Hutchinson and G. J. Milburn, *Journal of Modern Optics* **51**, 1211 (2009).
  - [6] B. H. Cumpston, S. P. Ananthavel, S. Barlow, D. L. Dyer, J. E. Ehrlich, L. L. Erskine, A. A. Heikal, S. M. Kuebler, I.-Y. S. Lee, D. McCord-Maughon, J. Qin, H. Rockel, M. Rumi, X.-L. Wu, S. Marder, and J. W. Perry, *Nature* **398**, 51 (1999).
  - [7] S. Kawata, H.-B. Sun, T. Tanaka, and K. Takada, *Nature* **412**, 697 (2001).
  - [8] A. Karotki, M. Drobizhev, Y. Dzenis, P. N. Taylor, H. L. Anderson, and A. Rebane, *Phys. Chem. Chem. Phys.* **6**, 7 (2004).
  - [9] I. Roy, T. Y. Ohulchanskyy, H. E. Pudavar, E. J. Bergey, A. R. Oseroff, J. Morgan, T. J. Dougherty, and P. N. Prasad, *J. Am. Chem. Soc.* **125**, 7860 (2003).
  - [10] S. Shafei and M. G. Kuzyk, *Phys. Rev. A* **88**, 023863 (2013).
  - [11] M. G. Kuzyk, *Phys. Rev. Lett.* **85**, 1218 (2000).
  - [12] M. G. Kuzyk, *Phys. Rev. Lett.* **90**, 039902 (2003).
  - [13] J. Zhou, U. B. Szafruga, D. S. Watkins, and M. G. Kuzyk, *Phys. Rev. A* **76**, 053831 (2007).
  - [14] D. S. Watkins and M. G. Kuzyk, *J. Chem. Phys.* **131**, 064110 (2009).
  - [15] D. S. Watkins and M. G. Kuzyk, *J. Chem. Phys.* **134**, 094109 (2011).
  - [16] T. Atherton, J. Lesnfsky, G. Wiggers, and R. Petschek, *J. Opt. Soc. Am. B* **29**, 513 (2012).
  - [17] C. J. Burke, T. J. Atherton, J. Lesnfsky, and R. G. Petschek, *J. Opt. Soc. Am. B* **30**, 1438 (2013).
  - [18] S. Shafei, R. Lytel, and M. G. Kuzyk, *J. Opt. Soc. Am. B* **29**, 3419 (2012).
  - [19] R. Lytel and M. G. Kuzyk, *Journal of Nonlinear Optical Physics & Materials* **22** (2013).
  - [20] R. Lytel, S. Shafei, J. H. Smith, and M. G. Kuzyk, *Phys. Rev. A* **87**, 043824 (2013).
  - [21] R. Lytel, S. M. Mossman, and M. G. Kuzyk, *J. Opt. Soc. Am. B* **33**, E14 (2016).
  - [22] R. Lytel, S. Mossman, E. L. Crowell, and M. G. Kuzyk, *Physical Review Letters* **119**, 073902 (2017).
  - [23] D. C. Rodenberger, J. R. Heflin, and A. F. Garito, *Phys. Rev. A* **51**, 3234 (1995).
  - [24] N. B. Vilas, B. Y. Wang, P. M. Rupasinghe, D. L. Maser, M. S. Safronova, U. I. Safronova, and P. K. Majumder, *Phys. Rev. A* **97**, 022507 (2018).
  - [25] V. E. Chernov, D. L. Dorofeev, K. I. Yu, and B. A. Zon, *J. Phys. B: At. Mol. Opt. Phys.* **38**, 2289 (2005).
  - [26] F. C. Grozema, R. Telesca, H. T. Jonkman, L. D. A. Siebbeles, and J. G. Snijders, *J. Chem. Phys.* **115**, 10014 (2001).
  - [27] M. Ponder and R. Mathies, *J. Phys. Chem* **87**, 5090 (1983).
  - [28] M. G. Kuzyk, *J. Chem Phys.* **125**, 154108 (2006).
  - [29] M. G. Kuzyk, *Phys. Rev. A* **72**, 053819 (2005).
  - [30] M. G. Kuzyk, *Nonlinear Optics and Quantum Op-*



- tics **46**, 159 (2015).
- [31] U. Eichmann, A. Sainz, S. Eilzer, T. Nubbemeyer, and W. Sandner, *Phys. Rev. Lett.* **110**, 203002 (2013).
- [32] J. Heckötter, M. Freitag, D. Fröhlich, M. Aßmann, M. Bayer, M. A. Semina, and M. M. Glazov, *Phys. Rev. B* **96**, 125142 (2017).
- [33] V. A. Yerokhin, S. Y. Buhmann, S. Fritzsche, and A. Surzhykov, *Phys. Rev. A* **94**, 032503 (2016).
- [34] M. S. O’Sullivan and B. P. Stoicheff, *Phys. Rev. A* **31**, 2718 (1985).
- [35] M. S. O’Sullivan and P. Stoicheff, *Phys. Rev. A* **33**, 1640 (1986).
- [36] J. E. Sansonetti, *J. Phys. Chem. Ref. Data* **35**, 301 (2006).
- [37] M. Gregoire, I. Hromada, W. F. Holmgren, R. Trubko, and A. D. Cronin, *Phys. Rev. A* **92**, 052513 (2015).
- [38] E. M. Landau, L. D. & Lifshitz, *Statistical Physics*, second revised english edition ed. (Pergamon Press, 1969).
- [39] X. Mi, J. V. Cady, D. M. Zajac, P. W. Deelman, and J. R. Petta, *Science* **355**, 156 (2017).
- [40] T. Hayashi, T. Fujisawa, H. D. Cheong, Y. H. Jeong, and Y. Hirayama, *Phys. Rev. Lett.* **91**, 226804 (2003).